TAT-BoNT/A$_{(1–448)}$, a novel fusion protein as a therapeutic agent: analysis of transcutaneous delivery and enzyme activity

Parvaneh Saffarian, Shahin Najar Peerayeh, Jafar Amani, Firooz Ebrahimi, Hamid Sedighian, Raheleh Halabian & Abbas Ali Imani Fooladi

Applied Microbiology and Biotechnology

ISSN 0175-7598
Volume 100
Number 6

Appl Microbiol Biotechnol (2016)
100:2785-2795
DOI 10.1007/s00253-015-7240-7

Springer

Appl Microbiol Biotechnol (2016) 100:2785–2795
DOI 10.1007/s00253-015-7240-7

APPLIED MICROBIAL AND CELL PHYSIOLOGY

TAT-BoNT/A$_{(1–448)}$, a novel fusion protein as a therapeutic agent: analysis of transcutaneous delivery and enzyme activity

Parvaneh Saffarian[1] · Shahin Najar Peerayeh[1] · Jafar Amani[2] · Firooz Ebrahimi[3] · Hamid Sedighian[2] · Raheleh Halabian[2] · Abbas Ali Imani Fooladi[2]

Received: 2 October 2015 / Revised: 2 December 2015 / Accepted: 5 December 2015 / Published online: 28 December 2015

Abstract Botulinum neurotoxin type A (BoNT/A) has been used as an injectable therapeutic agent for the treatment of some abnormal muscle contractions. In this study, TAT$_{(47–57)}$ peptide, a cell-penetrating peptide, was fused with the catalytic domain of BoNT/A for therapeutic purposes. HeLa and BE(2)-C cell lines were treated separately with purified TAT-BoNT/A$_{(1–448)}$ recombinant protein, and transduction of protein was analyzed by western blotting. Also, transcutaneous delivery through mouse skin surface was evaluated by immunohistochemistry. The in vitro catalytic activity of TAT-BoNT/A$_{(1–448)}$ was evaluated by HPLC. The presence of recombinant protein was detected in both of the cell lines as well as mouse skin cryosections after 60 and 120 min of incubation. The concentration of intracellular proteins was increased over time. HPLC analysis showed that this fusion protein has a biological activity 1.5 times as much as the full-length BoNT/A$_{(1–448)}$ protein. TAT-BoNT/A$_{(1–448)}$ fusion protein is biologically active and can transmit through living cells in vitro and in vivo successfully and more effectively compared with BoNT/A$_{(1–448)}$ protein as control.

Keywords Botulinum neurotoxin type A · Protein purification · TAT peptide · Fusion protein · Cell transduction · Transcutaneous delivery

✉ Shahin Najar Peerayeh
najarp_s@modares.ac.ir

✉ Abbas Ali Imani Fooladi
imanifouladi.a@gmail.com; imanifouladi.a@bmsu.ac.ir

[1] Department of Bacteriology, Faculty of Medical Sciences, Tarbiat Modares University, Tehran, Iran

[2] Applied Microbiology Research Center, Baqiyatallah University of Medical Sciences, Tehran, Iran

[3] Department of Biology, Faculty of Basic Sciences, Imam Hussein University, Tehran, Iran

Introduction

Clostridium botulinum produces a toxin called botulinum neurotoxin type A (BoNT/A) which is composed of three separate domains containing a binding, a translocating domain, and one catalytic domain (50 kDa each). The binding domain targets specific receptors on cholinergic neuron terminals. Then, the translocating domain helps the toxin into the neuronal cells via endocytosis (Lacy et al. 1998; Swaminathan and Eswaramoorthy 2000). After entry, the catalytic domain of the toxin acts as a zinc-dependent metalloprotease (Schiavo et al. 1992) and cleaves a protein located in synaptosomal junctions named SNAP-25 (synaptosomal-associated protein, 25 kDa) (Gul et al. 2010). This causes a temporary cessation in release of the stimulatory neurotransmitter mediators, acetylcholine in neuromuscular junctions. Therefore, the muscle contraction is disrupted. This property of the toxin is used for the treatment of some muscle disorders such as strabismus, blepharospasm, spasmodic, torticollis, cervical dystonia, or face wrinkles induced by aging process (Dhaked et al. 2010). Two BoNT serotypes (A and B) were the first toxins licensed as drugs for the treatment of human diseases. In January 2008, they were approved by the Food and Drug Administration (FDA) in the USA for clinical purposes (Dhaked et al. 2010). Since this biological drug is administered parenteral and injected mostly around the patient's face or neck that may make the patients uncomfortable. Also, the injection is sometimes associated with side effects such as tenderness, irritation, pain, burning, or numbness around the injected area. Hence, it is necessary to look for less invasive

ways for applying this useful drug. Because of the selective permeability of biological membranes, this toxin cannot freely transmit through the skin. Among various methods, use of cell-penetrating peptides (CPPs) is a favorable means to introduce biomolecules (peptides, proteins, or nucleotides) into cells. CPPs are composed of 3 to 30 peptide residues (De Coupade et al. 2005) which can freely pass through cell membranes. They can transport other cargoes such as plasmid DNA, siRNA, oligonucleotide, peptide-nucleic acid (PNA), peptides, proteins, and liposomes (Veerle and Cornelissen 2010). The conjugate can be in fusion with or non-covalently attached to cargo molecules.

To determine whether TAT peptide could deliver LC-BoNT/A through the skin, we constructed a conjugate (BoNT/$A_{(1–448)}$) by linking the amino acid sequences of TAT peptide (residues 47–57) to that of botulinum toxin type A catalytic domain by means of a hydrophobic linker. Transcutaneous delivery of purified fusion protein was evaluated in vitro and in vivo. Also, the biological activity of the chimeric protein was analyzed by HPLC. Our hypothesis was that the modification could facilitate the penetration of BoNT/$A_{(1–448)}$ into skin while its proteolytic activity for therapeutic purposes was preserved.

Materials and methods

Preparation of gene construct

A genomic construct (based on pET28a (+) expression vector) containing nucleic acid sequence of TAT-BoNT/$A_{(1–448)}$ was synthesized (GenScript, USA, Inc.) (Amani et al. 2014). Briefly, the construct was back-translated and optimized based on the bacterial expression host, *Escherichia coli*. Two parts of the fusion protein were linked by a hydrophobic linker (GSGSGS) and a 6 × His-tagged residue was added to carboxyl end of the protein to ease detection and purification. Two restriction enzyme sites were predicted on the 5′ and 3′ ends of TAT-BoNT/$A_{(1–448)}$ genomic sequence for *Bam*HI and *Hin*dIII enzymes, respectively. Restriction site of *Eco*RI was also inserted just upstream of BoNT/$A_{(1–448)}$ sequence. To ensure that each part of the chimeric protein maintained its natural structure and biological activity, the primary and secondary amino acid structure of TAT-BoNT/$A_{(1–448)}$ protein was studied in silico. Also, the 3-D structure of TAT-BoNT/$A_{(1–448)}$ protein was predicted by bioinformatics tools.

Expression vector containing nucleic acid sequence of TAT-BoNT/$A_{(1–448)}$ was cloned into the competent *E. coli* BL21 (DE3) (Novagen) as bacterial host. Finally, those bacterial colonies containing inserted peptide were cultured in LB broth containing kanamycin (100 μg/ml) to induce the protein expression.

Protein expression and purification

Five microliters fresh culture of appropriate clone of *E. coli* BL21 carrying inserted TAT-BoNT/$A_{(1–448)}$ was inoculated into 300 ml LB broth plus 100 μg/ml kanamycin and was incubated at 37 °C. Protein expression was induced by adding 0.5 mM isopropyl-b-D-thiogalactoside (IPTG) and 20 μM $ZnCl_2$ into the culture medium after reaching OD_{600} of about 0.6. Culture was incubated for 20–22 h at 18 °C while shaking at 180 rpm (Farasat et al. 2013; Jensen et al. 2003). The bacterial culture was centrifuged (8000×*g* for 6 min), and cell pellet was resuspended in lysis buffer (5 mM imidazole, 500 mM NaCl, 10 mM Tris–HCl) for 40 min. The lysed bacteria underwent sonication for 7 cycles with 45-s intervals on ice and centrifuged for 20 min at 4400×*g*. The supernatants of each clone were separated on SDS-PAGE and the bacterial clones with high expression rate were selected. Metal affinity chromatography was used to purify the protein.

Since the recombinant protein carried a His-tag (6 × His), the supernatant was collected after sonication and subjected to nickel-nitrilotriacetic acid (Ni^+-NTA) agarose resin (Qiagen) for purification. Briefly, supernatant was applied on the affinity chromatography and allowed to flow out of the column. Then, the column was washed with two consecutive washings (50 mM NaH_2PO_4 and 300 mM NaCl, pH 8.0) containing 20 and 100 mM imidazole, respectively. The nickel-bound proteins were finally eluted in a buffer containing 250 mM imidazole. As imidazole could interfere with protein stability, purified TAT-BoNT/$A_{(1–448)}$ protein was then transferred to 1 l of phosphate buffer (150 mM Na_2HPO_4, pH 7.0, 2 M NaCl) plus 10 % glycerol at 4 °C against three changes (two changes for 1 h and a last change overnight) through cellulose membrane dialysis tubing with a 10,000 molecular weight cutoff (10 K MWCO) (Sigma Aldrich, USA) (Held et al. 2010; Sepulveda et al. 2010).

In parallel, BoNT/$A_{(1–448)}$ protein was cloned and expressed using the same procedures and the purified protein was used as a control. In all experiments, purified recombinant BoNT/A protein was used.

Confirmation of recombinant protein

To confirm the expression of TAT-BoNT/$A_{(1–448)}$ recombinant protein, western blot analysis was conducted. After SDS-PAGE proteins were transferred onto the PVDF membrane using semi-dry blotting system (Bio-Rad, USA). Protein detection was performed by adding HRP-conjugated mouse anti-His-tag polyclonal IgG (Sigma, dilution 1:1000) for 2 h at room temperature with gentle shaking. After washing, DAB substrate (0.06 % in PBS, 10 μl H_2O_2) was added in the dark for 1–2 min to develop the specific protein bands.

Analysis of cell transduction

Purified TAT-BoNT/$A_{(1–448)}$ protein was tested in vitro for the ability to pass directly through living cultured cells. For this purpose, a monolayer of HeLa cells was prepared in a six-well cell plate (Kim et al. 2006) and incubated at 37 °C in a humidified atmosphere containing 5 % CO_2 to reach the confluency of about 80 %. The culture supernatant was replaced with 1 ml fresh RPMI medium (Gibco, USA), and then the cells were treated as follows: 3 μM purified TAT-BoNT/$A_{(1–448)}$ protein was added into two separate wells for 1 and 2 h, respectively; one well was treated with 3 μM purified LC-BoNT/A protein for 60 min and one well was left untreated, both as controls.

Also, for the first time, we analyzed the entry of TAT-BoNT/$A_{(1–448)}$ conjugates into the BE(2)-C neuroblastoma cell line. Like explained for the HeLa cell line, a monolayer of BE(2)-C cell line was prepared in a 6-well cell plate. After 24 h of incubation, the cell culture supernatant was replaced with 1 ml DMEM fresh medium (Gibco, USA). Then, the cells were treated as follows: 3 μM purified TAT-BoNT/$A_{(1–448)}$ protein was added into three separate wells and incubated for 30, 60, and 120 min, respectively. One well was treated with 3 μM of purified LC-BoNT/A for 120 min and one well was left untreated, both as controls. After the treatments, the cell culture supernatants (supposedly containing non-transduced proteins) were collected (Kim et al. 2011). The treated cells were collected in 20 mM trypsin-EDTA (Gibco, USA) at 37 °C for 5 min (30 s in case of BE(2)-C cells) followed by washing with phosphate-buffered saline (PBS). Harvested cells were lysed with complete Lysis-M kit (Roche, USA). The same volume of cell lysate and related culture supernatant from each well was loaded into SDS-PAGE gel followed by western blot analysis of the cellular protein extracts (Kim 2003; Ha et al. 2004). Band density was measured by Quantity One® software (Bio-Rad, USA).

Analysis of animal transcutaneous delivery

To investigate the transduction of TAT-BoNT/$A_{(1–448)}$ recombinant protein into epidermal cells of live animals, we applied certain concentrations of the recombinant protein on the skin surface of BALB/c mouse. For this purpose, five groups if mice were selected and housed with a fixed 12 h light/dark cycle with appropriate access to feed and water. The animal facility temperature was maintained at 23 °C with 60 % humidity. Procedures involving animals and their daily maintenance were in compliance with current international laws and policies (NIH Guide for the Care and Use of Laboratory Animals, NIH Publication No. 85-23, 1985, revised 1996). One micromolar TAT-BoNT/$A_{(1–448)}$ recombinant protein (50 μg) diluted in 100 μl PBS was sprayed topically onto the on 25 cm^2 circular area of mouse skin and allowed for certain period of time (30, 60, and 120 min) to be absorbed. LC-BoNT/A protein (50 μg) was applied on the skin surface of one group as control. The in vivo test was conducted in duplicate. The animals were then humanely sacrificed by cervical dislocation. The treated skins were removed, frozen, and prepared for histology from each mouse. The skin cryosections were analyzed with immunohistochemistry using HRP-conjugated anti-6 × His-tag anti-mouse polyclonal antibody (Sigma Aldrich, USA). This antibody visualizes the protein through the His-tag located at the N-terminal site of the TAT-BoNT/$A_{(1–448)}$. The antibody recognizes specifically the 6 × His-tag fused to either the amino or carboxyl terminus of targeted proteins in transfected cells. Peroxidase blocking (with 0.3 % H_2O_2) and protein blocking (with 1 % BSA) steps were applied on tissue sections to avoid non-specific protein signals.

To determine tissue variations we used hematoxylin and eosin (H&E) staining for skin cryosections exposed to the recombinant protein compared with the normal (untreated) mouse skin tissue.

In vitro analysis of TAT-BoNT/$A_{(1–448)}$ enzyme activity and functional analysis with HPLC

To assess the in vitro protease activity of TAT-BoNT/$A_{(1–448)}$, we conducted an enzyme assay using TAT-BoNT/$A_{(1–448)}$ and the natural substrate of BoNT/A toxin, SNAP-25.

A mixture of 200 nM TAT-BoNT/$A_{(1–448)}$ and 1 mM 17-residue SNAP-25 (187–203) in 50 μl of assay buffer (HEPES 30 mM, 5 mM DTT, 0.25 mM $ZnCl_2$, pH 6.0) was incubated at 37 °C for 5–260 min. The reaction was stopped with 0.09 ml of 0.7 % trifluoroacetic acid. Proteolytic cleavage of substrate was then evaluated by reversed-phase HPLC analysis Hi-Pore C18 column, 15 cm × 4.6 mm (Supelco). The reaction products were analyzed at 215 nm with Merit software (CECIL, Cambridge, UK). Solvent A was 0.1 % TFA and solvent B was 50 % acetonitrile/ 0.1 % TFA. The column was equilibrated with 25 % B. After sample injection, the column was held at 25 % B for 2.5 min, followed by a linear gradient to 75 % B in 15 min. The kinetic parameters of the 17-residue peptide for TAT-BoNT/$A_{(1–448)}$ and BoNT/A were calculated by Lineweaver–Burke plots with peptide concentrations ranging from 0.3 to 1.7 mM. The same reaction was designed and performed with the full-length native botulinum neurotoxin type A (BoNT/A) as control. Toxin activity was calculated for both TAT-BoNT/$A_{(1–448)}$ and native BoNT/A.

Results

Preparation of gene construct

Figure 1 demonstrates the schematic view of TAT-BoNT/$A_{(1–448)}$ construct and 3-D view of TAT-BoNT/A chimeric protein. The arrangement of designed TAT-BoNT/$A_{(1–448)}$ construct is

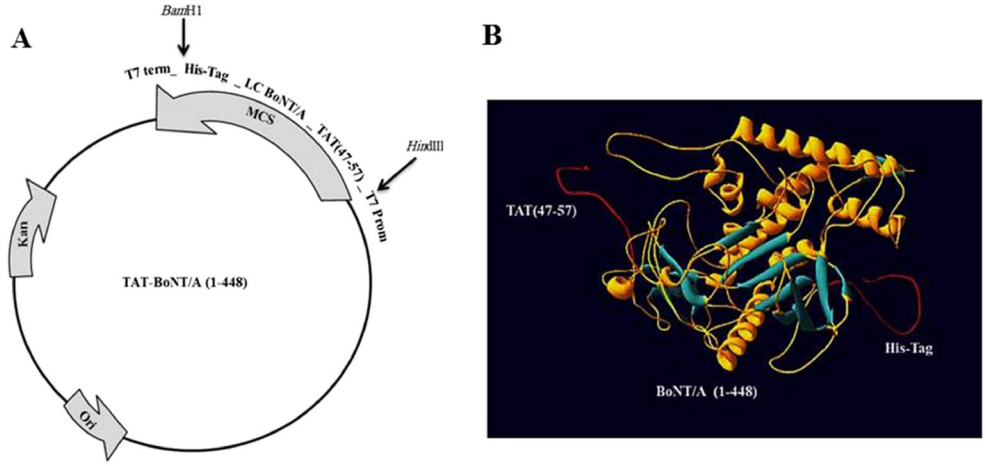

Fig. 1 **a** Schematic view of designed TAT-BoNT/$A_{(1–448)}$ construct based on pET28a expression vector. The order arrangement of the chimeric protein is shown on the *top* of multiple cloning sites. The sites of restriction enzymes are shown by *arrows*. **b** Three-dimensional view of TAT-BoNT/A chimeric protein. Three different parts of the chimeric protein have been marked as TAT peptide$_{(1–448)}$ and catalytic domain of botulinum toxin type A (which are connected by a hydrophobic linker) and His-tag (6 × His) that is added to the carboxyl end of this heterogeneous protein to ease detection. Both TAT peptide$_{(47–57)}$ and His-tag domains made two separated domains from the catalytic domain of the protein

presented in Fig. 1a. 3-D model analysis of TAT-BoNT/$A_{(1–448)}$ protein predicted that this engineered chimeric protein was composed of three separate parts. TAT peptide$_{(47–57)}$ and His-tag (6 × His) both were exposed on the surface of the chimeric protein and formed two separate parts which made them reachable for membrane targeting or protein detection, respectively (Fig. 1b). However, BoNT/$A_{(1–448)}$ which is responsible for protease activity of fusion protein was the core part of the recombinant protein. Figure 1 demonstrates the schematic view of designing TAT-BoNT/$A_{(1–448)}$ construct and 3-D view of TAT-BoNT/A chimeric protein. It does not include the docking data of TAT-BoNT/A with its substrate. The docking data of the fusion protein were presented in our previous work. The construct was accepted in gene bank with KF445072 accession number.

Expression and protein purification

Four clones of *E. coli* BL21(DE3) carried pET28a (+) containing TAT-BoNT/$A_{(1–448)}$ insertion sequence were selected to induce protein expression. The induction was performed using 0.5 mM IPTG at 18 °C overnight. Sonication was followed by high-speed centrifugation, and the supernatant containing soluble proteins was separated. Electrophoresis pattern of TAT-BoNT/$A_{(1–448)}$ fusion protein is shown in Fig. 5. One colony could express recombinant protein properly (54 kDa) as inclusion body.

Afterward, a large volume of recombinant protein was expressed in a 300-ml culture of the clone in LB broth containing 100 μg/ml kanamycin and IPTG (0.5 mM) was use as protein expression inducer. The bacterial culture was incubated at 18 °C for 20–22 h on a shaker at 150 rpm. Protein purification was performed using Ni-NTA agarose resin which specifically binds to the 6 × His-tag in the C-terminus of the protein. Proteins bound to the purification resin were eluted in buffer containing 250 mM imidazole. According to Fig. 2, the quantitative protein purity was measured about 90 % after purification using Image LabTM software with the Gel DocTM system. Also the protein concentration was measured by NanoDrop 2000 spectrophotmeter (Thermo

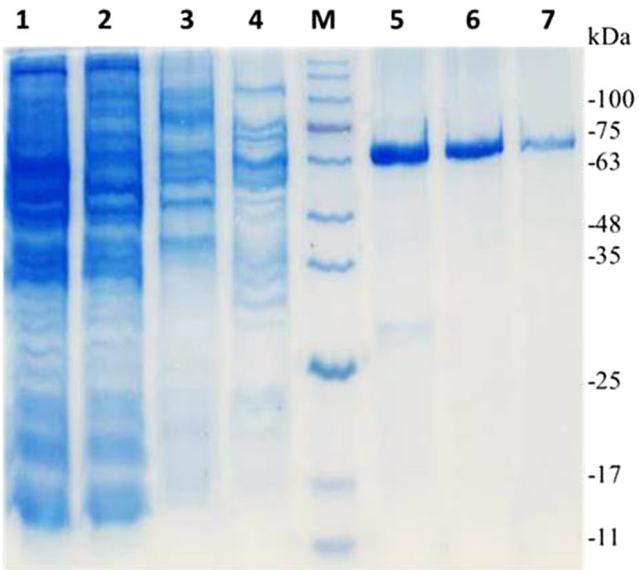

Fig. 2 Protein purification of TAT-BoNT/$A_{(1–448)}$ fusion protein. Induction was performed by 0.5 mM IPTG at 18 °C. SDS-PAGE electrophoresis stained with coomassie blue R250. *Lane 1*: before purification. *Lane 2*: flow. *Lanes 3* and *4*: washing with binding buffer containing 20 and 100 mM imidazole, respectively. *Lanes 5* and *6*: purified protein (54 kDa) eluted in buffer containing 250 mM imidazole (protein concentration was 0.5 mg/ml). *M*: prestained 10–170-kDa protein ladder (CinnaGen Co.)

Scientific™, USA) and Bradford method after purification. The purified protein concentration measured was about 0.5 mg/ml. The presence of TAT-BoNT/$A_{(1–448)}$ protein was confirmed by means of western blotting with HRP-conjugated anti-6 × His-tag rabbit anti-mouse monoclonal IgG (Sigma Aldrich, USA) (Fig. 3.). After purification, we investigated the entry of TAT-BoNT/$A_{(1–448)}$ protein into living cells over time in vitro and in vivo as explained bellow.

Analysis of cell line transduction

To test the delivery of purified TAT-BoNT/$A_{(1–448)}$ protein directly through living epidermal cell lines, a HeLa cell culture was used in a six-well cell plate. After treatments that were performed as described in material and methods section, the culture supernatants were collected. Cultured cells were lysed using Lysis-M solution (Roche, Manheim, Germany) after trypsinization. TAT-BoNT/$A_{(1–448)}$ recombinant protein was detected in HeLa cell extracts through western blotting using polyclonal HRP-conjugated anti-His-tag antibody. The density of protein band related to lysate samples was much more thicker from that of related supernatant samples; Which indicated that TAT-BoNT/$A_{(1–448)}$ protein can penetrate into the eukaryotic cells along different time intervals. As shown in Fig. 4, the band density of recombinant protein after 2 h was more than that of 1 h. This can be due to the fact that cell membrane penetration of TAT-BoNT/$A_{(1–448)}$ protein increases during incubation.

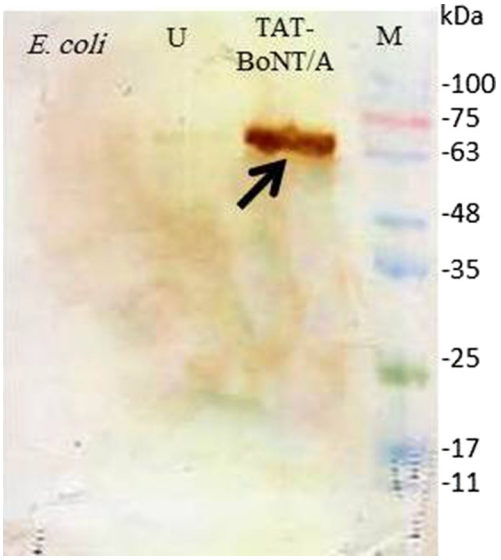

Fig. 3 Confirmation of purified TAT-BoNT/$A_{(1–448)}$ recombinant protein with western blotting. Western blot analysis by mouse anti-6 × His polyclonal IgG conjugated with HRP. The band of purified protein (54 kDa) is shown by *arrow*. Cell extract of *E. coli* Bl21 (DE3) lacking pET28a (+) was used as negative control (lane named *E. coli*). *U*: before induction. *M*: prestained 10–170-kDa protein ladder

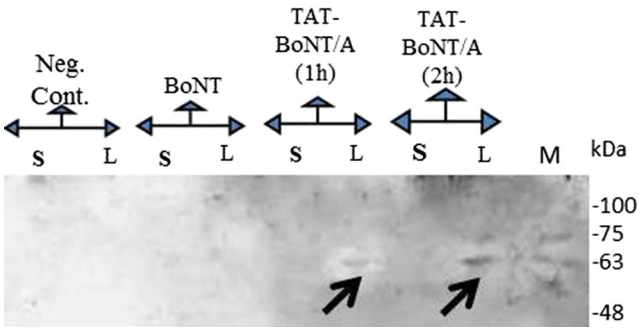

Fig. 4 Evaluating of transmembrane delivery of TAT-BoNT/$A_{(1–448)}$ recombinant protein with western blotting. Anti-His-tag antibody was detected TAT-BoNT/$A_{(1–448)}$ recombinant protein in HeLa cell lysate after 60 and 120 min. *TAT-BoNT/A (1 h)* and *(2 h)*: cell culture treated with TAT-BoNT/$A_{(1–448)}$ protein after 1 and 2 h, respectively. *BoNT*: cell culture treated with LC-BoNT/A protein as control. *S*: culture supernatant. *L*: cell lysate. *Neg. Cont.*: normal cell culture lysate and supernatant as negative control

Entry of TAT-BoNT/$A_{(1–448)}$ conjugates into the BE(2)-C cell line

To assess the ability of TAT-BoNT/$A_{(1–448)}$ recombinant protein for passing directly through living neuronal cells, six-well plate culture of BE(2)-C neuroblastoma cell line was treated with purified protein for various time periods (30, 60, and 120 min). As shown in Fig. 5, the internalized proteins were traced by HRP-conjugated polyclonal anti-His-tag antibody and visualized with western blotting. The signs of recombinant protein penetration were observed after 30 min and the band related to the penetrated TAT-BoNT/$A_{(1–448)}$ into the cells after 120 min was denser than the one after 60 and 30 min, respectively. This suggested a time-dependent penetration of protein into living cells.

Analysis of animal transcutaneous delivery

We applied 100 μl PBS solution containing 1 μM TAT-BoNT/$A_{(1–448)}$ recombinant protein on the skin surface of BALB/c mouse in different time intervals. Figure 6a, b, e, f, i, j, m, n demonstrated that TAT-BoNT/$A_{(1–448)}$ could penetrate into epidermal cells after 30 min. While LC-BoNT/A showed no skin penetration even after 120 min. Protein transduction increased over time, and protein aggregates of 120-min treatment in skin cryosections were increasingly more than those of 30 and 60 min, respectively. Also, Fig. 6c, d, g, h, k, l, o, p demonstrates tissue changes before and after treatment with TAT-BoNT/$A_{(1–448)}$ and LC-BoNT/A compared with the normal untreated tissue. The results show no signs of alterations including infiltration of inflammatory cells or tissue damage even after 120 min of treatment with TAT-BoNT/$A_{(1–448)}$ recombinant protein.

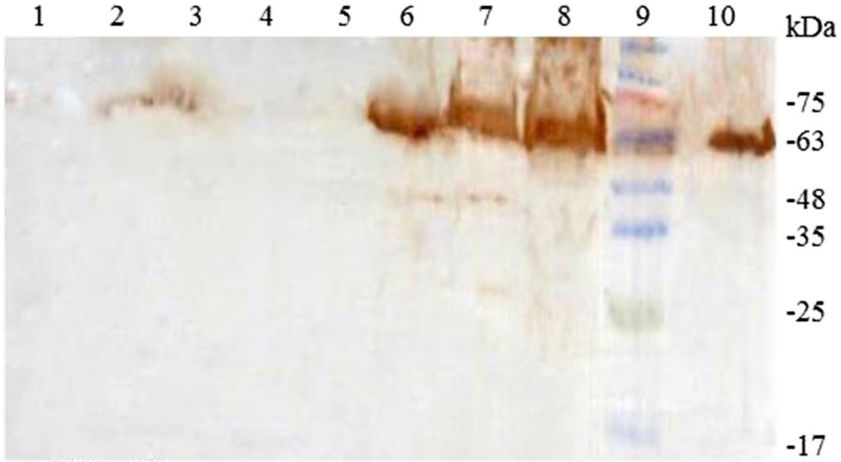

Fig. 5 Evaluating of transmembrane delivery of TAT-BoNT/$A_{(1–448)}$ recombinant protein with western blotting. Anti-His-tag antibody detected TAT-BoNT/$A_{(1–448)}$ recombinant protein in BE(2)-C cell lysate after 30, 60, and 120 min. Description of columns are as follow. *1*: culture supernatant of untreated cells. *2*: culture supernatant of cells treated with LC-BoNT/A. *3*: culture supernatant of cells treated with TAT-BoNT/$A_{(1–448)}$ recombinant protein after 120 min. *4*: cell lysates of untreated cells. *5*: cell lysates of cells treated with LC-BoNT/A. *6*, *7*, *8*: cell lysates of cells treated with TAT-BoNT/$A_{(1–448)}$ recombinant protein after 30, 60, and 120 min, respectively. *9*: protein size marker. *10*: purified TAT-BoNT/$A_{(1–448)}$

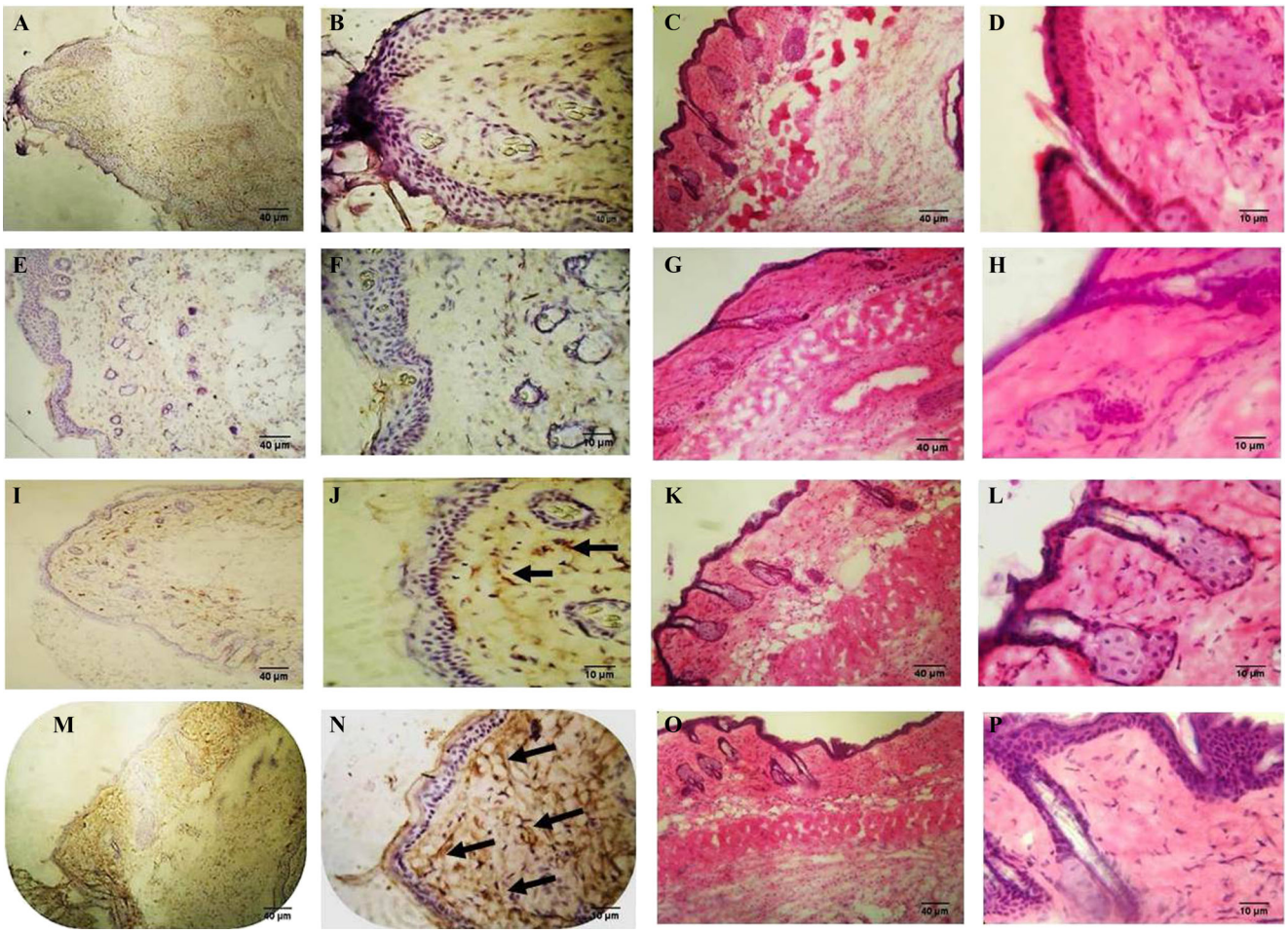

Fig. 6 In vivo analysis of transduction of TAT-BoNT/$A_{(1–448)}$ protein through mouse skin. **a**, **b**, **e**, **f**, **i**, **j**, **m**, **n** Immunohistochemistry staining of mouse skin cryosections. **c**, **d**, **g**, **h**, **k**, **l**, **o**, **p** Hematoxylin-eosin staining of mouse skin cryosections. **a**–**d** Untreated normal mouse skin. **e**–**h** Mouse skin treated with LC-BoNT/A as control. **i**–**l** Mouse skin treated with TAT-BoNT/$A_{(1–448)}$ protein for 60 min. **m**–**p** Mouse skin treated with TAT-BoNT/$A_{(1–448)}$ protein for 120 min. ×40 and ×10 magnitudes are presented for each view. The *arrow* shows some points that TAT-BoNT/$A_{(1-448)}$ stained with anti-6×His-tag antimouse polyclonal antibody and it penetrate into penetrate into epidermal cells

Overall, the penetration of TAT-BoNT/A fusion protein was evaluated by western blotting in cultured cell lines after 2 h. Also, the entry of protein into mouse skin was followed up by immunohistochemistry for 60 and 120 min. After this time, no significant histological changes were observed in tissue section treated with TAT-BoNT/$A_{(1–448)}$ (H&E staining) in comparison with normal untreated skin (Fig. 6).

In vitro analysis of TAT-BoNT/$A_{(1–448)}$ enzyme activity

We conducted an enzyme assay using TAT-BoNT/$A_{(1–448)}$ and the natural substrate of BoNT/A toxin, SNAP-25 to assess the in vitro protease activity of TAT-BoNT/$A_{(1–448)}$ recombinant protein. After incubation in a 50-μl assay volume at 37 °C for 20 and 260 min, the fractions related to fragmented substrate were detected with HPLC (Fig. 7). By reducing the peak area of substrate in HPLC chromatograms, the peak area of cleavage fragments of substrate were growing by increasing the reaction time. As a control, the enzymatic activity of the full-length BoNT/A toxin was calculated under the same condition using 1.7 mM substrate (Fig. 8). Figure 9 depicted the Lineweaver–Burke plots of the 17-residue peptide (187–203) for TAT-BoNT/$A_{(1–448)}$ with concentrations ranging from 0.3 to 1.7 mM. In contrast to TAT-BoNT/$A_{(1–448)}$, the full-length BoNT/A toxin showed no enzymatic activity in substrate concentrations less than 1.7 mM at an assay time less than 260 min. However, the recombinant protein had protease activity on substrate concentration of 0.3 mM at assay time as low as 20 min. Proteolytic activity of both TAT-BoNT/A and BoNT/A had positive correlation with the amount of the substrate (0.3–1.7 mM) in the reaction mixture.

The calculated initial activity of TAT-BoNT/$A_{(1–448)}$ recombinant protein was ~6 μM/min while the activity of the full-length BoNT/A toxin was 1.3 μM/min. Other kinetic parameters (K_m and k_{cat}) are shown beside the plot. K_m and k_{cat} related to full-length BoNT/A was ~4 μM and 0.9 s^{-1}, respectively. These data corresponded with other similar studies conducted on LC- BoNT/A and BoNT/A (Gul et al. 2010). The results of calculating the kinetic parameters of TAT-BoNT/$A_{(1–448)}$ recombinant protein in comparison with the full-length BoNT/A are summarized in Table 1.

Discussion

Because of the high molecular weight of BoNT/A toxin, intact skin is impermeable to direct penetration of this macromolecule. However, Carmichael et al. (2010) used the first transdermal delivery system of BoNT/A to reduce plasma extra vacation (PE), a critical component of the inflammatory response. They found that effective transdermal delivery of BoNT/A through intact skin could be facilitated by co-

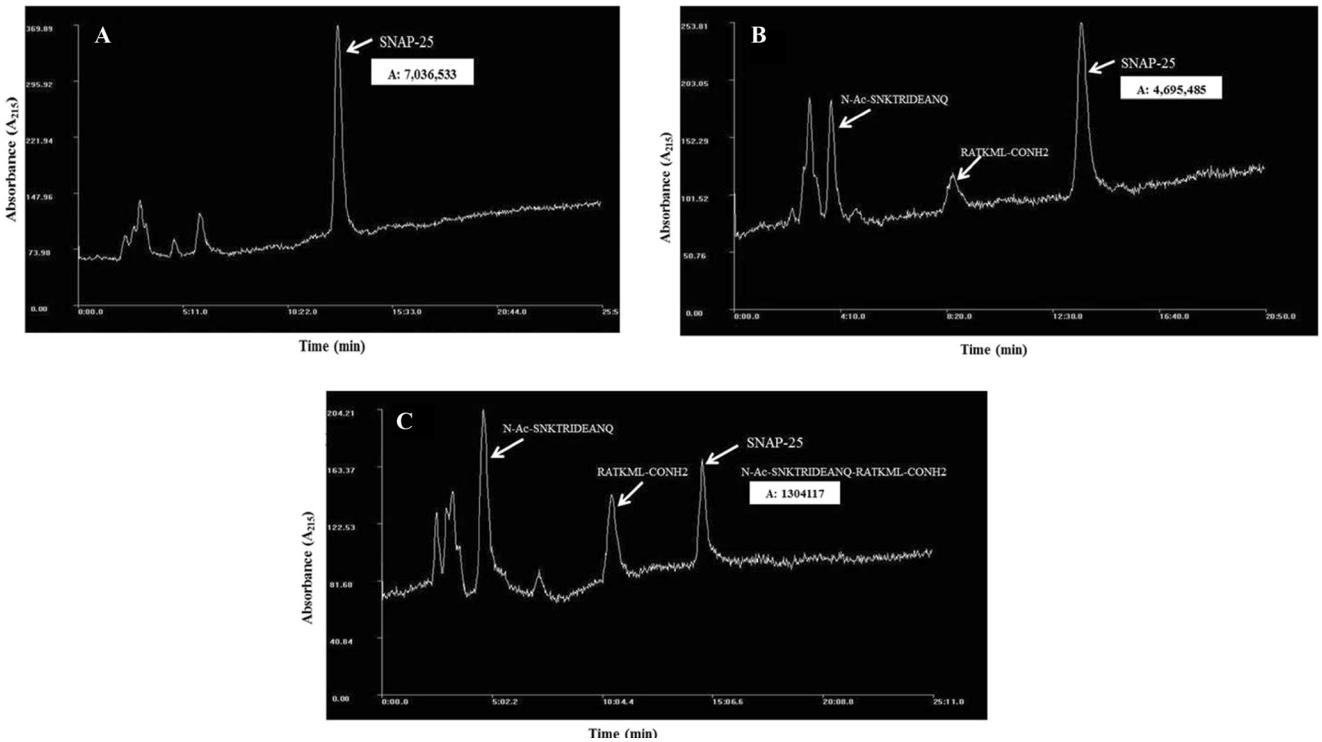

Fig. 7 In vivo analysis of TAT-BoNT/$A_{(1–448)}$ proteolysis activity on 17-residue SNAP-25 (1 mM) by HPLC. Chromatogram of reaction mixture **a** before enzyme assay and **b** after 20 min and **c** after 260 min of incubation at 37 °C. The peak area related to intact substrate is shown in *boxes*. The first three peaks represent the solvent front (<4 min) and reduced DTT (7 min) in the reaction mixture. The sequence of substrate and the products were determined by MS–MS and are shown in the *panels*

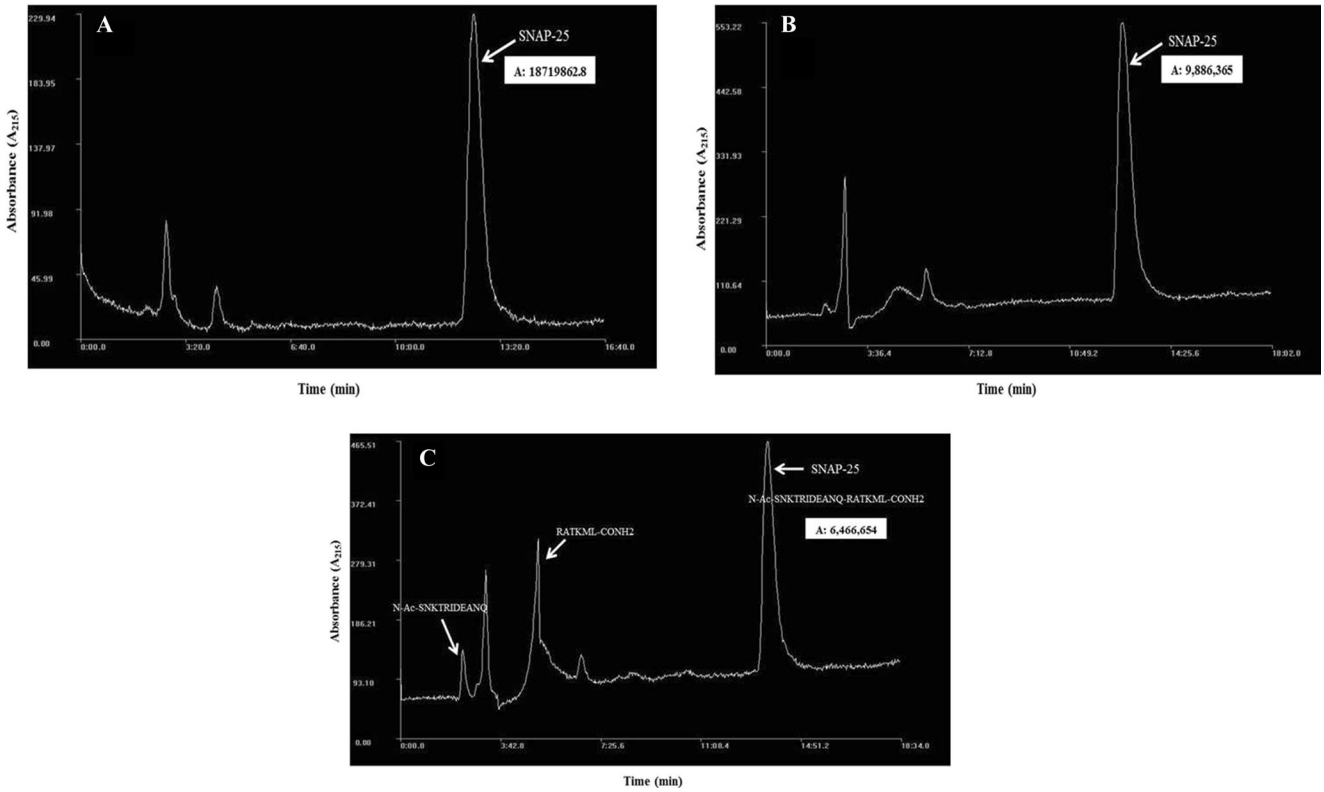

Fig. 8 In vivo analysis of proteolysis activity of the full-length native BoNT/A on 17-residue SNAP-25 (1.7 mM) by HPLC. Chromatogram of reaction mixture **a** before enzyme assay and **b** after 20 min and **c** after 260 min of incubation at 37 °C. The peak area related to intact substrate is shown in *boxes*. The first three peaks represent the solvent front (<4 min) and reduced DTT (7 min) in the reaction mixture. The sequence of substrate and the products were determined by MS–MS and are shown in the *panels*

administration of a short synthetic peptide (TD-1) and BoNT/A to the mouse hind paw.

In this study, the TAT peptide (residues 47–57) was directly fused to LC-BoNT-A (residues 1–448) to form a single recombinant protein. Designing a fusion protein may require some structural modifications and requires a lower doses upon administration for non-covalent binding (Kamei et al. 2008) and has the advantage of being safer in administration and is more economical. According to some studies (Thomas et al. 2010; Amani et al. 2014), 1:1 ratio covalent cargo–CPP complexes could be more dependent on free CPP properties than non-covalent CPP-cargo complexes. Electron microscope images of fluorescently labeled transporters have been shown that these recombinant proteins are in intimate contact with cell membrane and directly transfer through intact cutaneous barrier (Rothbard et al. 2000).

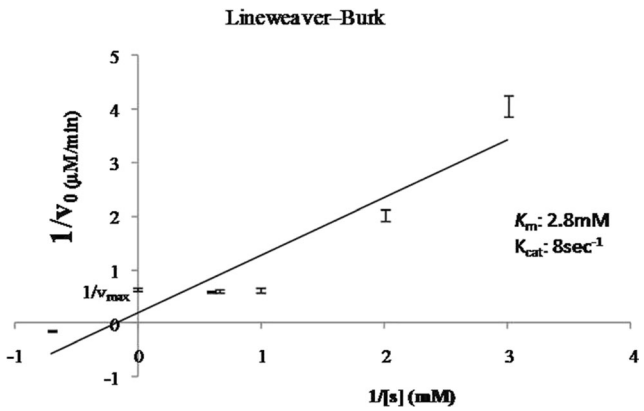

Fig. 9 Lineweaver-Burk plots for TAT-BoNT/$A_{(1–448)}$ recombinant protein hydrolyses of 17-residue SNAP-25. In the plot, *1/[s]* is the reciprocal of the substrate concentration (in mM^{-1}) and *1/v* is the reciprocal of the initial hydrolysis rate (in mM^{-1}/min). The kinetic parameters (K_m and k_{cat}) obtained from this experiment are shown next to the plot

TAT-BoNT/$A_{(1–448)}$ protein is very hydrophobic (the charge of both BoNT/A light chain and $TAT_{(47–57)}$ peptide is highly positive with PI of 9.2) (Amani et al. 2014). This recombinant protein expresses as inclusion body when induced with 1 mM IPTG and incubated at 37 °C (Jensen et al. 2003; Ahmed and Smith 2000). Therefore, it is necessary to use

Table 1 Kinetic parameters of TAT-BoNT/$A_{(1–448)}$ recombinant protein in comparison with the full-length BoNT/A

	*K*m (μM)	Activity (μM/min)	k_{cat} (s^{-1})	The catalytic efficiency (k_{cat}/K_m), ($\mu M^{-1}/s^{-1}$)
TAT-BoNT/$A_{(1–448)}$	2.8	6	8	2.8
LC-BoNT/A	4	4	0.9	0.2

solubilizing agents such as urea, arginine, glycerol or surfactants such as Tween-20 in order to reduce protein aggregation during purification (Lee et al. 2006). Despite the high expression level of recombinant proteins in form of inclusion body, proteins should become unfolded. This may decrease the biological activity during the refolding into native conformation (e.g., use of urea gradient). Also, protein refolding process is time consuming and uneconomical, especially in case of large-scale protein production. Therefore, it is necessary to apply a reliable and cost-effective way for production of recombinant proteins with a structure more similar to the native protein. In this study, the abovementioned concern was addressed through induction of protein expression with low levels of IPTG (0.5 mM) and incubation of bacterial culture at low temperatures (18 °C) (Moe et al. 2009). These conditions make bacterial cells express the protein gradually avoiding formation of inclusion bodies. Zinc ion ($ZnCl_2$) was added to the bacterial cell culture, because it plays an important role in the maintenance of physical structure and biological activity (Lacy and Stevens 1999). Using low temperature for expression and purification using traditional column chromatography methods, we obtained a noticeable quantity of TAT-BoNT/$A_{(1–448)}$ recombinant protein.

Protein transduction domains (PTD) are short hydrophobic cationic peptides which have the ability to pass through membranes of living cells by interaction with phospholipid bilayer (Pooga et al. 1998; Soomets et al. 2000). Internalization occurs through different, yet unknown, mechanisms and depends on both the type of peptide and the cell culture model. Distinct cellular distribution patterns of common investigated CPPs may offer a potential for localized epithelial delivery and they lack the ability for systemic drug delivery across epithelial layer. Also, there is evidence that upon injection, the BoNT/A protein does not diffuse beyond 2 cm, exerting its paralyzing activity around the injection site with very limited spreading (Trehin et al. 2004; Costa et al. 2012). In this study, we sprayed TAT-BoNT/A solution directly on mouse skin and as expected the diffusion of protein was much less than when it was administered as an injectable drug. Also, there is a miniscule potential of systemic spread of TAT-BoNT/A through skin.

Together with this information, what make this technology so attractive are the high rate of uptake, the ability of carrying therapeutically useful amount of drug, and the depth of skin penetration (Rothbard et al. 2000). On the other hand, among different CPPs, those with moderate cell uptake such as TAT peptide$_{(47–57)}$, are more desirable than those with high transportation rate (e.g., transport and penetrate in) for carrying molecules into biological membranes, because the former enter cells trough endocytosis and therefore do not disrupt the cell membrane integrity (Mueller et al. 2008). In this study, the cell membrane transduction of TAT-BoNT/$A_{(1–448)}$ recombinant protein was tested in vitro and in vivo in comparison with the full-length BoNT/A. As shown by Jeong et al. (2008), the intracellular concentration of Tat-CK (human brain creatine kinase) fusion protein gradually increased with increasing incubation periods which is in consistent with our results both in cell culture (eukaryotic epithelial and neuronal cells) and mouse skin. Here, we have introduced the TAT peptide as a cell-penetrating peptide which facilitates the transport across the cutaneous barrier when applied topically to mouse skin. The results of similar studies demonstrated that the properties of the transporter were not adversely affected by the addition of the protein cargo (Rothbard et al. 2000).

Activity of the purified TAT-BoNT/A recombinant protein was calculated to be approximately 6-fold greater than that of the native toxin, fulfilling our goal of providing very active, highly pure recombinant protein. Like the full-length BoNT/A which has been shown in other studies to be stable for several hours under assay conditions (Schmidt and Bostian 1995), the TAT-BoNT/A recombinant protein has proteolytic activity for more than 4 h (260 min) during essay time as well. The full-length BoNT/A showed a lower activity rate in this study than what was tested in other studies. However, Schmidt and Bastian et al. have shown that BSA enhanced the initial rate of hydrolysis of 17-residue SNAP-25 by full-length BoNT/A mediated (Schmidt and Bostian 1997). However, we decided not to use any enzyme stimulator to simulate the natural condition for enzyme activity. There is a large body of evidence indicating the crucial role of DTT and $ZnCl_2$ inactivity enhancement of this Zn-metalloprotease (10–20 %) (Rawat et al. 2008). Hence, we added low concentrations of DTT and $ZnCl_2$ to the assay buffer (30 mM HEPES) to facilitate proteolytic activity of the enzyme. The amount of calculated k_{cat} for TAT-BoNT/$A_{(1–448)}$ was about 8 times as much as the full-length BoNT/A while the K_m value of BoNT/A was affected to a somewhat lesser degree and was decreased by a factor of 1.4. One possible reason could be that in the form of light chain alone, the active site of the BoNT/A is more accessible to the substrate because of the lack of structural interactions made by two other toxin domains. Also, the catalytic efficiency of TAT-BoNT/$A_{(1–448)}$, calculated as k_{cat}/K_m (2.8 $\mu M^{-1}/s^{-1}$) is ~14-fold higher than that of its full-length version, BoNT/A, in this study (0.2 $\mu M^{-1}/s^{-1}$).

According to the literature, K_m reflects binding affinity between substrate and enzyme, while the catalytic rate constant, k_{cat}, defines the capability of enzyme catalytic site for converting the maximum number of substrate molecules to product per unit of time (a turnover rate) (Wang and Liang 1994; Schmidt and Bostian 1997). So, it can be concluded that with the lower amounts of k_{cat}, less amounts of enzyme is needed for substrate hydrolysis over a time unit. It is an advantage because the administration of lower drug in further clinical applications can be safer and causes less possible unexpected effects. The data resulted from this study indicates that fusion of LC-BoNT/A to TAT allowed internalization into

living cells effectively with no further cell membrane manipulation. We demonstrated that TAT-BoNT/$A_{(1–448)}$ recombinant protein can freely penetrate both into the cultured eukaryotic epithelial (Whelan et al. 1992), neuronal [BE(2)-C] cell lines, and mouse skin (in vivo). Also, making a LC-BoNT/A conjugate increased the potential for proteolytic activity compared to full-length BoNT/A. Peptide-mediated delivery of BoNT/A is an easy and non-invasive way of administering the drug that may prove to be useful for therapeutic purposes in clinical practices.

Acknowledgments This article was extracted from thesis and was supported with Applied Microbiology Research Center Baqiyatallah University of Medical Sciences and Department of Bacteriology, Faculty of Medical Sciences Tarbiat Modares University. We thank Dr. Mohammad Bagher Salehi for providing HPLC analysis and assistance during enzyme assay experiments.

Compliance with ethical standards

Funding This study was not funded by any grant from any institute.

Conflict of interest The authors declare that they have no competing interests.

Ethical approval All animal experimentation was performed according to the guidelines of the Baqiyatallah University Animal Care with prior approval of the Institutional Animal Care.

References

Ahmed SA, Smith LA (2000) Light chain of botulinum A neurotoxin expressed as an inclusion body from a synthetic gene is catalytically and functionally active. J Protein Chem 19(6):475–487

Amani J, Saffarian P, Najar Peerayeh S, Imani Fooladi AA (2014) Designing and analyzing the structure of Tat-BoNT/A(1–448) fusion protein: an in silico approach. Mol Biol Res Commun 3(2):13

Carmichael NM, Dostrovsky JO, Charlton MP (2010) Peptide-mediated transdermal delivery of botulinum neurotoxin type A reduces neurogenic inflammation in the skin. Pain 149(2):316–324

Costa A, Pegas Pereira ES, de Oliveira Pereira M, Calixto dos Santos FB, Favaro R, Stocco PL, Favaro de Arruda LH (2012) Comparative study of the diffusion of five botulinum toxins type-A in five dosages of use: are there differences amongst the commercially-available products? Dermatol Online J 18(11):2

De Coupade C, Fittipaldi A, Chagnas V, Michel M, Carlier S, Tasciotti E, Darmon A, Ravel D, Kearsey J, Giacca M, Cailler F (2005) Novel human-derived cell-penetrating peptides for specific subcellular delivery of therapeutic biomolecules. Biochem J 390(Pt 2):407–418

Dhaked RK, Singh MK, Singh P, Gupta P (2010) Botulinum toxin: bioweapon & magic drug. Indian J Med Res 132:489–503

Farasat A, Ebrahimi F, Mousavy J, Salehi MB, Rostamian M (2013) Characterization of antibody titer and immunogenic feature of light chain of botulinum neurotoxin type A. Ann Biol Res 4(3):5

Gul N, Smith LA, Ahmed SA (2010) Light chain separated from the rest of the type a botulinum neurotoxin molecule is the most catalytically active form. PLoS One 5(9):e12872

Ha KT, Lee YC, Cho SH, Kim JK, Kim CH (2004) Molecular characterization of membrane type and ganglioside-specific sialidase (Neu3) expressed in *E. coli*. Mol Cells 17(2):267–273

Held DM, Shurtleff AC, Fields S, Green C, Fong J, Jones RG, Sesardic D, Buelow R, Burke RL (2010) Vaccination of rabbits with an alkylated toxoid rapidly elicits potent neutralizing antibodies against botulinum neurotoxin serotype B. Clin Vaccine Immunol 17(6):930–936

Jensen MJ, Smith TJ, Ahmed SA, Smith LA (2003) Expression, purification, and efficacy of the type A botulinum neurotoxin catalytic domain fused to two translocation domain variants. Toxicon 41(6):691–701

Jeong MS, Kim DW, Lee MJ, Lee YP, Kim SY, Lee SH, Jang SH, Lee KS, Park J, Kang TC, Cho SW, Kwon OS, Eum WS, Choi SY (2008) HIV-1 Tat-mediated protein transduction of human brain creatine kinase into PC12 cells. BMB Rep 41(7):537–541

Kamei N, Morishita M, Eda Y, Ida N, Nishio R, Takayama K (2008) Usefulness of cell-penetrating peptides to improve intestinal insulin absorption. J Control Release 132(1):21–25

Kim CH (2003) A Salmonella typhimurium rfaE mutant recovers invasiveness for human epithelial cells when complemented by wild type rfaE (controlling biosynthesis of ADP-L-glycero-D-mannoheptose-containing lipopolysaccharide). Mol Cells 15(2):226–232

Kim DW, Kim SY, An JJ, Lee SH, Jang SH, Won MH, Kang TC, Chung KH, Jung HH, Cho SW, Choi JH, Park J, Eum WS, Choi SY (2006) Expression, purification and transduction of PEP-1-botulinum neurotoxin type A (PEP-1-BoNT/A) into skin. J Biochem Mol Biol 39(5):642–647

Kim M, Kim HY, Kim S, Jung J, Maeng J, Chang J, Lee K (2011) A protein transduction domain located at the NH2-terminus of human translationally controlled tumor protein for delivery of active molecules to cells. Biomaterials 32(1):222–230

Lacy DB, Stevens RC (1999) Sequence homology and structural analysis of the clostridial neurotoxins. J Mol Biol 291(5):1091–1104

Lacy DB, Tepp W, Cohen AC, DasGupta BR, Stevens RC (1998) Crystal structure of botulinum neurotoxin type A and implications for toxicity. Nat Struct Biol 5(10):898–902

Lee SH, Carpenter JF, Chang BS, Randolph TW, Kim YS (2006) Effects of solutes on solubilization and refolding of proteins from inclusion bodies with high hydrostatic pressure. Protein Sci 15(2):304–313

Moe ST, Thompson AB, Smith GM, Fredenburg RA, Stein RL, Jacobson AR (2009) Botulinum neurotoxin serotype A inhibitors: small-molecule mercaptoacetamide analogs. Bioorg Med Chem 17(8):3072–3079

Mueller J, Kretzschmar I, Volkmer R, Boisguerin P (2008) Comparison of cellular uptake using 22 CPPs in 4 different cell lines. Bioconjug Chem 19(12):2363–2374

Pooga M, Hallbrink M, Zorko M, Langel U (1998) Cell penetration by transportan. FASEB J Off Publ Fed Am Soc Exp Biol 12(1):67–77

Rawat R, Ashraf Ahmed S, Swaminathan S (2008) High level expression of the light chain of botulinum neurotoxin serotype C1 and an efficient HPLC assay to monitor its proteolytic activity. Protein Expr Purif 60(2):165–169

Rothbard JB, Garlington S, Lin Q, Kirschberg T, Kreider E, McGrane PL, Wender PA, Khavari PA (2000) Conjugation of arginine oligomers to cyclosporin A facilitates topical delivery and inhibition of inflammation. Nature Med 6(11):1253–1257

Schiavo G, Rossetto O, Santucci A, DasGupta BR, Montecucco C (1992) Botulinum neurotoxins are zinc proteins. J Biol Chem 267(33):23479–23483

Schmidt JJ, Bostian KA (1995) Proteolysis of synthetic peptides by type A botulinum neurotoxin. J Protein Chem 14(8):703–708

Schmidt JJ, Bostian KA (1997) Endoproteinase activity of type A botulinum neurotoxin: substrate requirements and activation by serum albumin. J Protein Chem 16(1):19–26

Sepulveda J, Mukherjee J, Tzipori S, Simpson LL, Shoemaker CB (2010) Efficient serum clearance of botulinum neurotoxin achieved using a pool of small antitoxin binding agents. Infect Immun 78(2): 756–763

Soomets U, Lindgren M, Gallet X, Hallbrink M, Elmquist A, Balaspiri L, Zorko M, Pooga M, Brasseur R, Langel U (2000) Deletion analogues of transportan. Biochim Biophys Acta 1467(1):165–176

Swaminathan S, Eswaramoorthy S (2000) Structural analysis of the catalytic and binding sites of *Clostridium botulinum* neurotoxin B. Nat Struct Biol 7(8):693–699

Thomas A, Lins L, Divita G, Brasseur R (2010) Realistic modeling approaches of structure-function properties of CPPs in non-covalent complexes. Biochim Biophys Acta 1798(12):2217–2222

Trehin R, Krauss U, Beck-Sickinger AG, Merkle HP, Nielsen HM (2004) Cellular uptake but low permeation of human calcitonin-derived cell penetrating peptides and Tat(47–57) through well-differentiated epithelial models. Pharm Res 21(7):1248–1256

Veerle K, Cornelissen B (2010) Targeting the tumour: cell penetrating peptides for molecular imaging and radiotherapy. Pharmaceuticals 3(3):20

Wang W, Liang TC (1994) Substrate specificity of porcine renin: P1', P1, and P3 residues of renin substrates are crucial for activity. Biochemistry 33(48):14636–14641

Whelan SM, Elmore MJ, Bodsworth NJ, Brehm JK, Atkinson T, Minton NP (1992) Molecular cloning of the *Clostridium botulinum* structural gene encoding the type B neurotoxin and determination of its entire nucleotide sequence. Appl Environ Microbiol 58(8):2345–2354